Reprinted from Preprint Volume: Eleventh Conference on Severe Local Storms, Kansas City, Missouri, October 2-5, 1979. Published by the American Meteorological Society, Boston, Mass.

OBJECTIVES, OPERATION, AND RESULTS OF PROJECT NIMROD

T. Theodore Fujita

The University of Chicago
Chicago, Illinois

1. INTRODUCTION

Damaging winds on the ground which are induced by thunderstorms have been classified as either "tornado" or "straight-line wind". This classification is based on the presumption that gusty, straight-line winds rush out of the subcloud layer of severe thunderstorms.

Straight-line winds, in relation to gust fronts, were investigated extensively by Goff (1975) who found that a gust front may extend outward more than 20 km from the source thunderstorm.

Some 30 years ago, Faust (1947) made an extensive survey of forests near Frankfurt, Germany, finding that there were a number of swaths and pockets of high winds. A few years later, Müldner (1950) mapped in detail the directions of tree falls after a squall-line passage. His map revealed the existence of the four distinct centers of diverging damage directions, each of which was characterized by severe damage on trees.

Investigation of the Eastern 66 accident at JFK International Airport, New York City by Fujita (1976) and Fujita and Byers (1977) led to a conclusion that the three centers of diverging winds had moved across the approach end of the runway. The term "downburst" was introduced in designating the downdraft accompanied by an outburst of damaging wind on the ground. Since then more cases of aircraft accidents have been analyzed by Fujita and Caracena (1977).

During 1976 and 1977 Fujita and his collaborators at the University of Chicago launched extensive aerial survey missions over Midwestern corn fields after severe thunderstorms. The aim of the missions was to map directions and intensities of damaging winds made visible by the corn crops.

Of 142 downbursts mapped photogrammetrically, 47% were rated as F0; 32%, F1; 19%, F2, and 1%, F3. The smallest downburst was less than one mile long, while the longest was over 30 miles. Several small downbursts were embedded inside the overall area of a large downburst. This is somewhat like finding several suction-vortex swaths inside the overall area of a large tornado.

A small downburst with a damage length of P2 (3.1 miles) or less is, thus, called a "microburst". The distinction of microburst from downburst permits us to identify the microburst damage inside the downburst damage. For details, refer to "Manual of Downburst Identification" by Fujita (1978).

One could relate a tornado with a downburst, each of which is accompanied by damaging winds on the ground. A funnel cloud up in the air is not called a "tornado" unless it is accompanied by damaging wind on the ground. Likewise, a downdraft, no matter how strong it may be in mid-air, should not be identified as a "downburst" unless an outburst of damaging wind (F0 or stronger) is confirmed on the ground (see Figures 1, 2, and 3).

Table 1. The FPP (Fujita-Pearson) wind scale applicable to both tornado and downburst. From Fujita (1971), and Fujita and Pearson (1973). For review of the scale, refer to Abbey (1976).

Scale	F Windspeed	P Damage length	P Damage width
0	40 - 72 mph	0.4 - 0.9 mile	6 - 17 yds
1	73 - 112	1.0 - 3.1	18 - 55
2	113 - 157	3.2 - 9.9	56 - 175
3	158 - 206	10 - 31	0.1 - 0.3 mile
4	207 - 260	32 - 99	0.4 - 0.9
5	261 - 318	100 - 316	1.0 - 3.1
6	-----	-----	3.2 - 9.9
7	-----	-----	10.0 - 31.6

Corn stalks utilized as no-cost indicators of downburst winds. Photo by Duane Stiegler one week after a F0 downburst in Illinois.

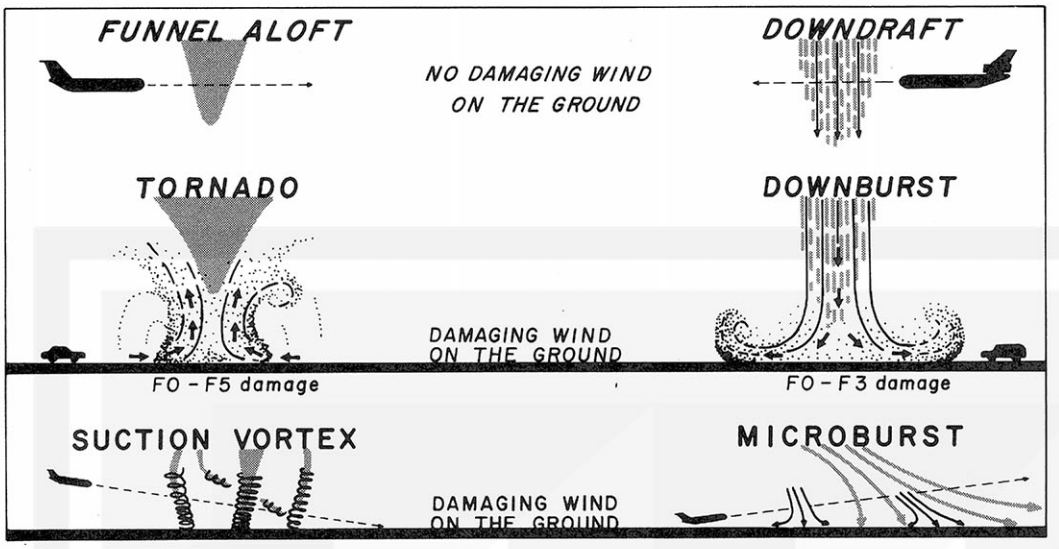

Figure 1. Diagrams showing the comparable features of tornado and downburst.

Most tornadoes and downbursts travel rather fast, necessitating the addition of the translational velocity to obtain their actual wind fields.

COMPARATIVE DEFINITIONS OF TORNADO AND DOWNBURST

FUNNEL ALOFT

A cone- or rope-shaped column of cloud pendant from a convective cloud base. No damaging wind is experienced on the ground beneath a passing funnel cloud. The F P P scale is not assigned to a funnel cloud, because there is no damage on the ground.

DOWNDRAFT

Relatively small-scale current of air with marked downward motion. Downdraft is encountered inside or below the cloud, but it does not induce a damaging wind on or near the ground. No F P P scale is assigned to a downdraft.

TORNADO

A violently-rotating column of air, pendant from a cumulonimbus or a towering cumulus, which induces a damaging wind on the ground. Tornado is accompanied by a funnel cloud and/or a swirling column of dust and debris. The F P P scale of tornadoes varies between 0,0,0 and 5,5,5.

DOWNBURST

A localized current of air descending from the base of a cumulonimbus cloud, which induces an outward burst of damaging wind on or near the ground. Some form of precipitation accompanies a downburst. The F P P scale of downbursts varies between 0,2,5 and 3,5,7.

SUCTION VORTEX

A fast-spinning column of air embedded inside a much-larger, parent circulation. Suction vortex is observable as a column of spinning dust and/or small funnel cloud if its parent vortex is relatively free from dust and debris. The F P P scale of suction vortices varies between 0,0,0 and 5,0,2.

MICROBURST

A mini-size downburst occurring with or without downburst. By virtue of its small horizontal dimensions, a microburst induces a strong wind shear near the surface, often resulting in head and tail winds within less than a mile. The F P P scale of microbursts varies between 0,0,0 and 2,1,5.

Figure 2. Suction vortices of all sizes and shapes inside the Wichita Falls, 1979 tornado. Copyrighted photo by Floyd Styles.

Figure 3. A microburst in Kansas on July 1, 1978. One of eight copyrighted photos by Mike Smith, showing the entire life of the storm.

2. KESSLER - FUJITA CONTROVERSY

During the past several years, there has been both agreement and disagreement between Kessler and Fujita, with regard to tornadoes and downbursts.

Since I pointed out the downburst phenomenon, several storm researchers at NSSL and at the University of Oklahoma have on various occasions stated, in effect, that there has been little evidence of downbursts in Oklahoma, and the downburst winds may well be those experienced quite often along the leading edge of an advancing gust front.

Fujita does not share this view at all, because he has obtained a large number of aerial photographs showing the traces of localized diverging flow, one to 10 miles across, superimposed upon the overall area of straight and parallel-line winds, which are likely to be caused by gust fronts.

It is hard to imagine that the pattern of downburst wind can be mapped in Oklahoma, through a ground survey in particular, where even the trace of a weak tornado in the chase-team movie cannot be found easily from the ground as well as from the air. Winter wheat in western Oklahoma is too flexible and too short to be disturbed by a 50 mph wind at the tree-top level. Bushes and trees are grown to live with the low-level jet of 50 to 60 mph gusts experienced often in Oklahoma in the spring.

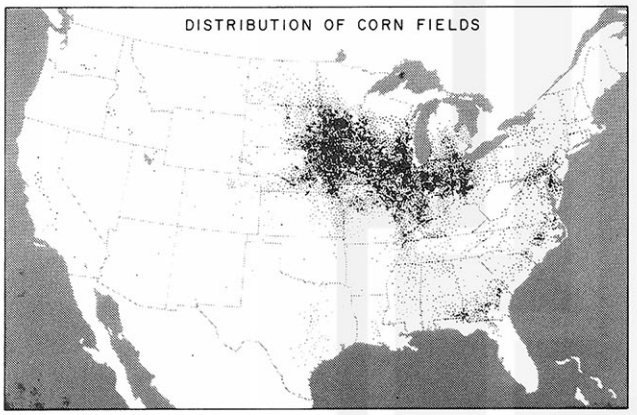

Figure 4. Corn crops are extremely responsive to F0 to F1 winds. Their broad leaves remain tilted under F0 winds causing a differential scattering of the sunlight, making visible from the air the wind effects of weak vortex and microburst for a couple of days. The whole stalks lean under F1 winds, but they grow back upright becoming ready for the next storm.

Corn fields, on the other hand, respond extremely well to a wind of 50 mph or faster. Figure 4 shows the distribution of corn fields which yield 64% of the world's supply of corn. Numerous corn stalks in the corn belt are the no-cost indicators of maximum winds. Most of the signatures of down- and microbursts were found and photographed from low-flying aircraft over these corn fields.

If the NSSL network were surrounded by extensive corn fields, convincing evidence of downbursts could have been found in Oklahoma a long time ago.

The high-quality research on dual-, triple-, and multiple-Doppler measurements at NSSL which led to the recent papers by Ray (1976) (1978) and Brandes (1977) (1978) and others revealed the structure of Oklahoma thunderstorms. Nevertheless, the evidence of "inconsistency" against case studies, no matter how extensive they may be, should not be used as the basis of the "rejection" of any proposed mechanism. It is because the past case studies at NSSL and elsewhere as well are still limited to specific periods of specific thunderstorms.

More research on different thunderstorms in various parts of the country by different researchers may come up with other mechanisms. An example of a caved-in top of a mesocyclone over the NIMROD network showed an evidence in support of the long descent of the air from the cloud top to near the ground (refer to further descriptions in this paper).

3. NIMROD NETWORK AND OPERATIONS

The Project NIMROD network was placed just to the west of Chicago, Illinois where ample corn crops were grown annually. The operation period of May 15 through June 30 was chosen as it is the growing season for corn which is used as the high-wind indicators.

In view of the existence of a horseshoe-shaped hill consisting of the terminal moraine of the ice-age glacier, the CHILL radar was placed at the top of the hill. ORD is located inside the hill and YKV, atop a local pile of the moraine. The base-line lengths of the Doppler triangle are

YKV to CHL ... 59.69 km
CHL to ORD ... 57.86 km
ORD to YKV ... 56.04 km

Geographic coordinates of these radars are given in Table 2.

Table 2. Locations of three Doppler radars at Yorkville (YKV), O'Hare International Airport (ORD) and near Monee (CHL).

Radars	Latitudes	Longitudes	Heights
YKV (CP-3)	41° 37'05"N	88°24'10"W	740 ft
ORD (CP-4)	41° 57'23"N	87° 54'10"W	660 ft
CHL (CHILL)	41° 27'12"N	87°43'19"W	790 ft

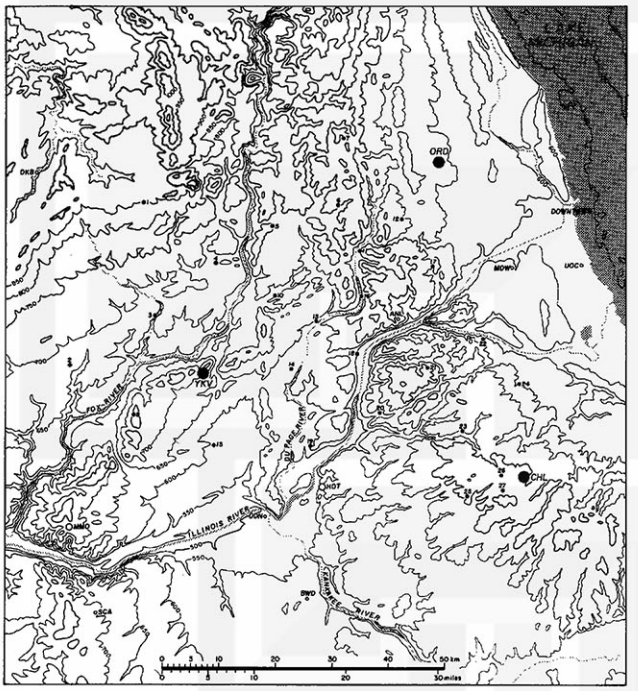

Figure 5. Topography of the NIMROD (Northern Illinois Meteorological Research On Downburst) network and vicinity. An arc-shaped hill across the network is the remnant of the ice-age glacier which had receded into Lake Michigan.

27 PAM stations were distributed in and around the Doppler triangle (see Figure 5).

The network operations were directed by Fujita at the YKV Command Post. Ramesh Srivastava and Greg Forbes were at the site of the HOT radar, which was operated in the multi-elevation PPI mode 24 hours a day.

Through radio and telephone communications with Fujita at YKV, the scanning modes of the triple Doppler radars were determined and requested by Srivastava and Forbes always using the "3-minute" cycle time.

Both reflectivity and velocity fields on the CP-3 color display were recorded on 35-mm slides. At the conclusion of the operation, 15,000 color slides were obtained and filed.

PAM data were received and taped at YKV where wind-field maps were produced at 15-minute intervals by Roger Wakimoto. These maps were of vital importance in the decision making by Fujita.

About 200 rawinsondes were released at 30- to 60-minute intervals from the YKV site. The release times and the maximum tracking heights were determined based on the storm situation. More than 20 balloons were tracked downward after their bursts.

During the 45 days of the network operation, we obtained various types of data: (1) downburst- and tornado-inducing bow echoes, (2) two mesocyclone echoes with caved-in tops, (3) isolated downbursts and microbursts with up to 70 mph winds, and (4) a number of gust fronts.

This paper includes the preliminary results of items (1) and (2) with evidence of the avalanche of air descending from the cloud top to near the ground.

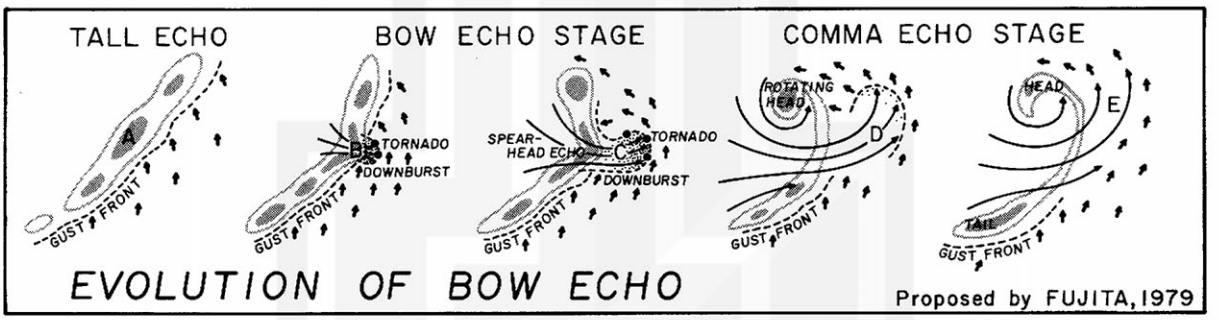

Figure 6. A model of the evolution of bow echo. Bow echo in this new model is produced by a downburst thunderstorm as it snowballs, or cascades down to the ground. This model is contrary to Fujita's(1978) first thought, "bow echo produces downbursts". The final stage of this evolotion is a comma echo which can be identified on PPI scope quite often.

4. BOW-ECHO PRODUCED BY DOWNBURST

Since Nolen (1950) identified the "line echo wave pattern, LEWP", forecasters have been using this specific echo pattern as a guide for warning of high winds.

Hamilton (1970) pointed out that a "bulge" in LEWP is closely related to high winds on the ground. Prior to the NIMROD operation, Fujita (1978) called the bulged echo the "bow echo", identifying its final stage as the "comma echo". In these studies, a bulge of echo was regarded as an "inducer of high wind".

The preliminary research of NIMROD data is going to reverse this "chicken and egg" relationship. Fujita's 1979 model of bow-echo evolution highlights the downburst as the cause of the bulge or the bow.

The model in Figure 6 shows that the bow is caused by the downburst, instead. Namely, a downburst is already in progress when a line echo takes the shape of a bow.

CP-3 at YKV recorded the life history of this phenomena from 15 minutes before the downburst to its end. At 1250 CDT, one of the strongest echoes in a line began showing 15 m/s Doppler velocity away from the radar. In 10 minutes, at 1300 CDT, a trench in the reflectivity pattern formed and an area of high Doppler velocity dashed out of the weak-echo trench (see Figures 7 and 8 and refer to Stage B in Figure 6).

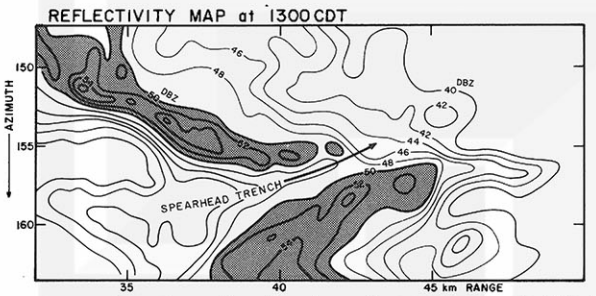

Figure 7. A weak-echo trench appeared on the 3.5° scan of the YKV radar. The height of the scan cone at the location of the trench is about 2.5 km.

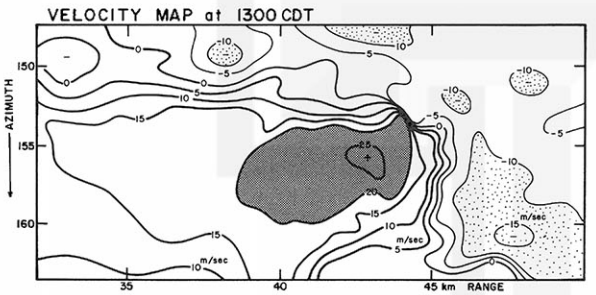

Figure 8. Velocity field in the B-scan area of above figure. An area of 26 m/sec dashed out of the trench, producing 2 tornadoes on its front.

At 1314 CDT, a 2-mile wide tongue of 28 to 31 m/s wind was pushing out violently. An F1 tornado formed at 1310 CDT on the leading edge, killing one person. This time corresponds to Stage C (see Figures 6 and 9).

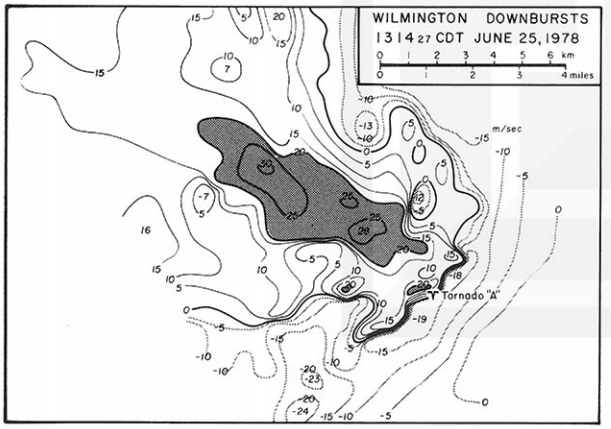

Figure 9. Isodop pattern viewed from YKV, showing a 2-mile wide swath of 20 m/sec winds. Tornado "A" formed at 1310 CDT.

A post-storm damage survey by Forbes revealed that there were three microbursts embedded inside an F1 downburst. Two tornadoes with F0 and F1 intensities formed along the leading edge of the downburst.

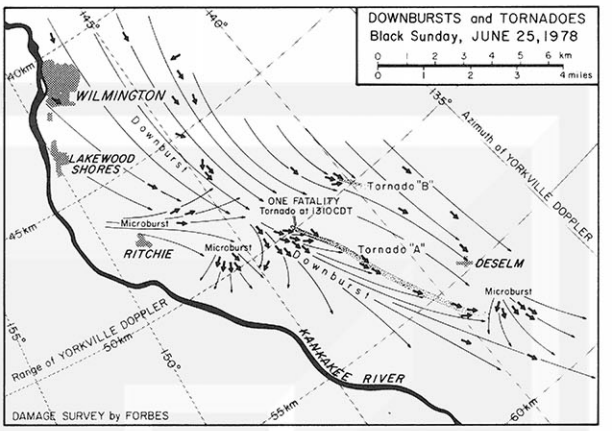

Figure 9-A Downbursts and microbursts confirmed on the ground throgh aerial survey by Forbes. The FPP of two tornadoes are 0,0,1 and 1,1,2.

The Doppler velocity field at 1321 - 1324 CDT, corresponding to Stage D in Figure 6, shows the existence of a 30 to 60 kt airflow converging toward the downburst area which had moved out of its parent echo (see Figure 10).

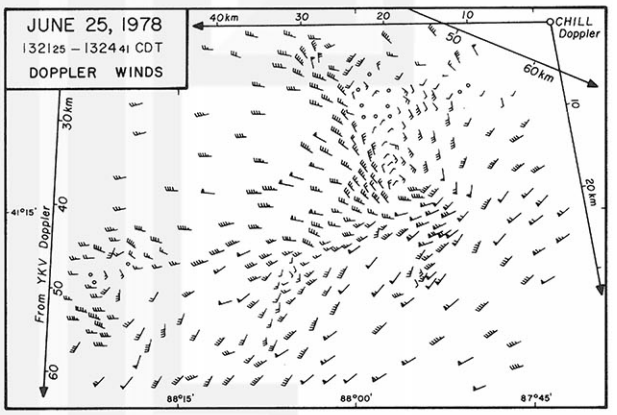

Figure 10. Doppler winds, one barb 10 kt and one flag 50 kt, computed from isodop fields in Figures 11 and 12. It is seen that the air behind the line converges into the downburst thunderstorm as it snowballs down to the ground. Dual Doppler data covering the entire evolution period are now being analysed at the University of Chicago.

The isodops, isolines of equal Doppler velocity, from YKV and CHL at identical time and height are quite different from each other (see Figures 11 and 12).

The YKV radar kept scanning at the 3.5° elevation angle. The isodops in Figure 11 are on a scan cone slanted toward the southeast. The height over the downburst area is about 3 km AGL.

The CHL isodops in Figure 12 were obtained by combining the velocities near the intersections of successive scan cones.

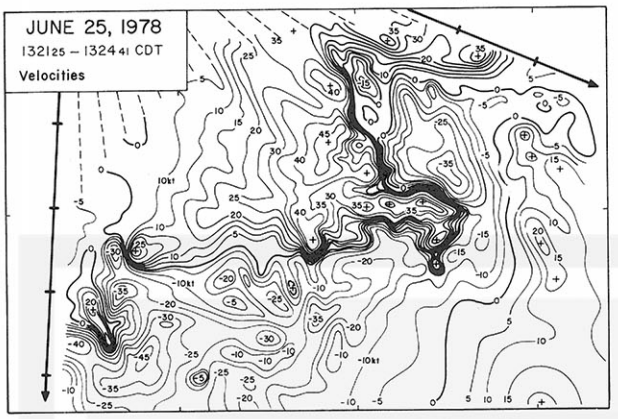

Figure 11. Isodops in kt viewed from YKV. An extremely tight velocity gradient marks the leading edge of the high winds at about 3 km AGL.

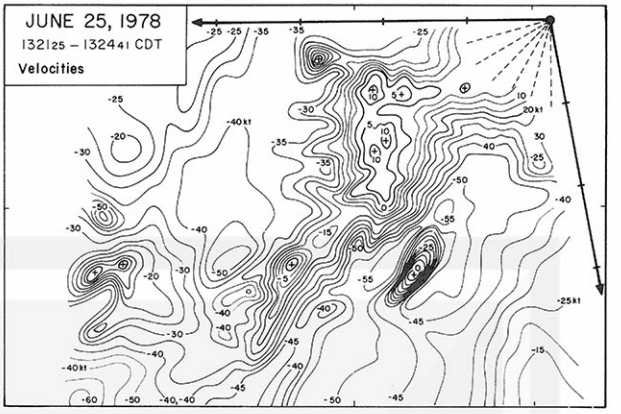

Figure 12. Isodops at the same time and height as viewed from CHL. The leading edge of high wind is not identifiable, despite its definite existence, due to the bad direction of view.

A detailed analysis of the dual-Doppler data, which is being performed, holds the key in answering the question, "Does an overgrown thunderstorm suddenly collapse to the ground, leaving behind a mesoscale circulation, inside of which a line echo deforms into a bow echo and finally into a comma echo?"

From an energetic point of view, it is quite plausible that the potential energy stored at the cloud top through the overshooting processes is converted suddenly into the kinetic energy of the descending air. Incloud evaporation of entrained droplets of all sizes, along with the entrainment of dry air from behind the storm, will permit a long descent of the air from the cloud top to near the ground.

The downburst airflow associated with a bow echo is most likely to be the result of a snowballing collapse of a majestic thunderstorm. Apparently, an overgrown thunderstorm suddenly reverses its airflow direction upside-down, upon reaching a critical point of no return.

Table 3. Examples of bow echoes which induced downbursts and/or tornadoes. Storm identifications are:- EARL (Earlville, IL), PHIL (Phillips, WI), SPGF (Springfield, IL), and WILM (Wilmington, IL). The Wilmington storm was scanned by dual Doppler radars.

Storms	EARL	PHIL	SPGF	WILM
DATES	6/30/77	7/4/77	8/6/77	6/25/78
TIME OF STORMS				
Began, CST	0810	1220	1430	1150
Ended, CST	0930	1540	1740	1300
Duration	1hr 20m	3hr 20m	3hr 10m	1hr 10m
DOWNBURSTS				
Number	10	25	10	3
Max F scale	F1	F2	F1	F1
TORNADOES				
Number	5	none	18	2
Max F scale	F3	--	F3	F1

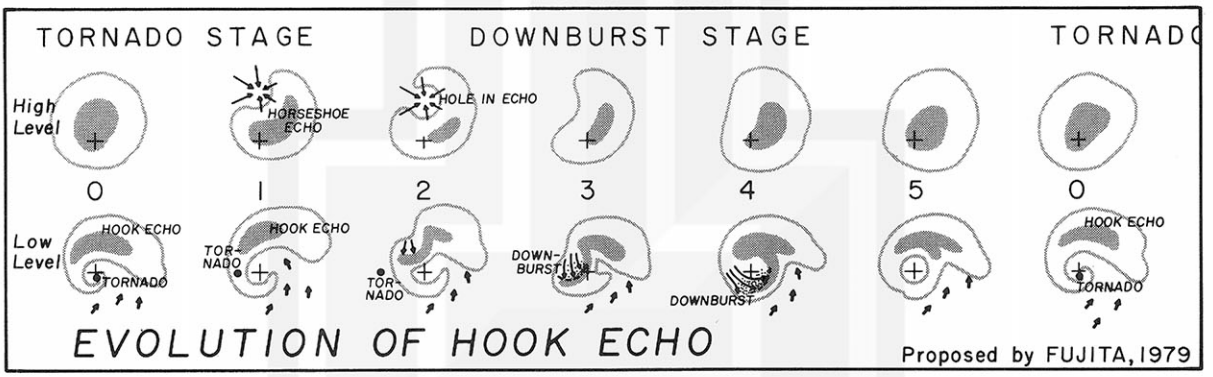

Figure 13. A model of cyclic evolution of hook echo. As tornado weakens in Stages 1 and 2, it moves slower than the parent cell, turning into a slanted rope funnel attached to the cloud. The descending air triggered at the horseshoe- and hole-echo level reaches the ground as a twisting downburst.

5. HOOK-ECHO INDUCED DOWNBURST

Since the hook echo photographed by the Illinois State Water Survey on April 9, 1953, echoes with hook configurations have been regarded as the parent cloud of intense tornadoes.

Forbes (1977) reported that 65% of the 55 echoes with hook, circulation, or appendage produced tornadoes. Based on the PPI tilt sequences, Lemon (1977) identified the tornado-producing phase of mesocyclones not to be the peak updraft phase, but the increasing downdraft phase which is consistent with earlier papers by Fujita (1973), Lemon et al. (1975), Brandes (1977), and Burgess et al. (1977).

Fujita's 1979 model in Figure 13 shows the evolution of a supercell mesocyclone storm with alternating stages of tornado and downburst formations. These stages are

Stage 0 ... Updraft decreases; a tornado forms inside the hook and moves with the hook

Stage 1 ... Onset of the sinking cloud top; tornado weakens, moving slower than the parent cloud

Stage 2 ... Echo top caves in; strong downdraft distorts the low-level echoes; rope-shaped tornado is left behind the cloud.

Stage 3 ... Tornado dies; downburst winds begin swirling around the mesocyclone center

Stage 4 ... Peak intensity of twisting downburst; updraft increases

Stage 5 ... Updraft reaches its peak with the maximum cloud top height

Stage 0 ... New cycle of evolution begins with the formation of a tornado

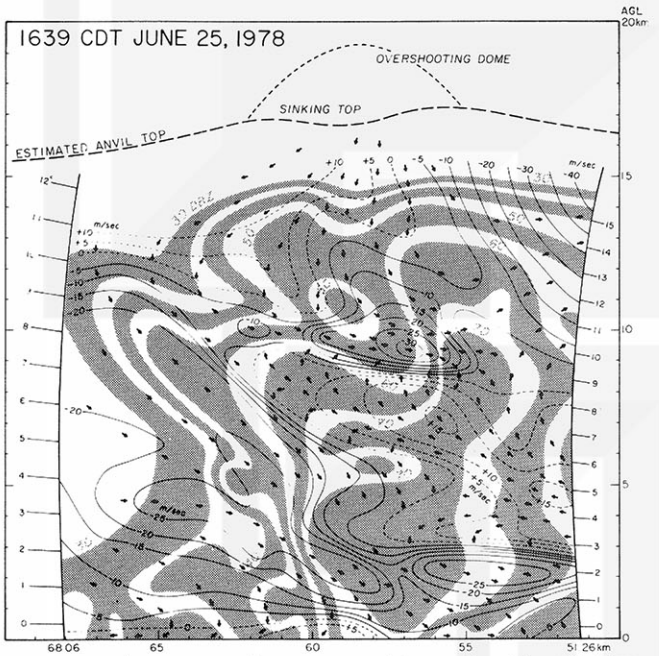

Figure 14. Vertical cross section of reflectivity (5 DBZ intervals) superimposed upon the velocity field toward(-) and away(+) from CHL.

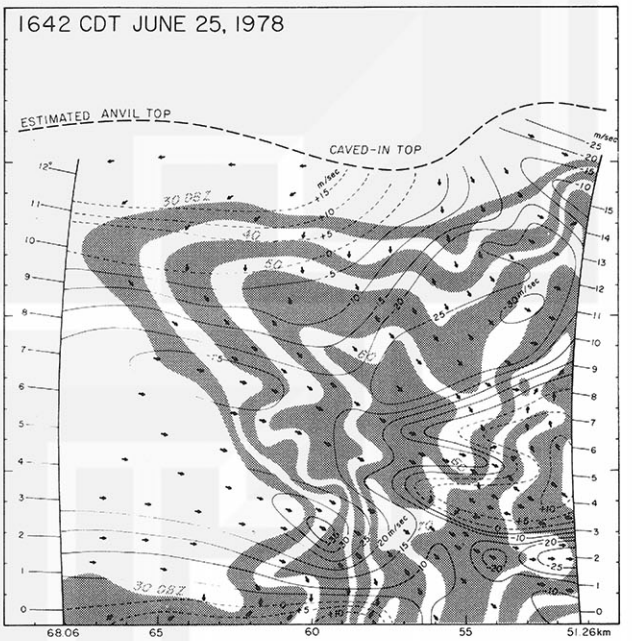

Figure 15. Within only three minutes, the reflectivity isopleths beneath the caved-in top sunk to 5-km AGL. Arrows are estimated flow directions.

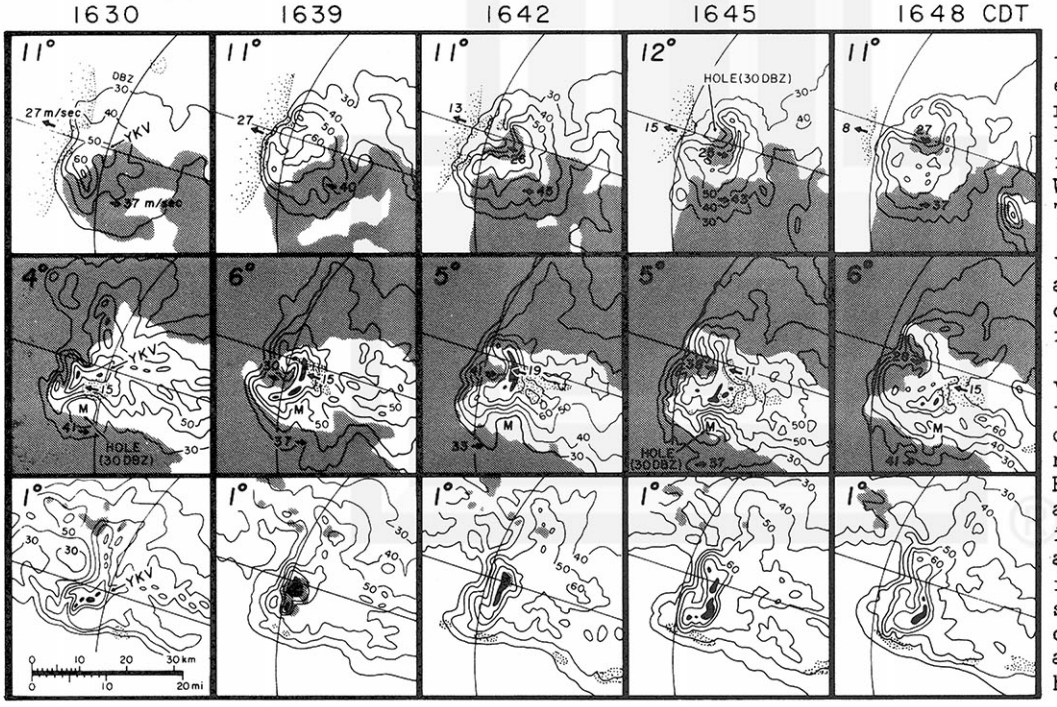

Figure 16. Evolution of the Hook echo in above Figures. CP-3 at YKV was looking upward continuously. Refer to Wilson and Fujita(1979) in this volume.

Dotted areas denote +5 m/s or faster and shaded, -20 m/s or faster velocity from CHL.

Pockets of high velocity near the top are the fast-descending air turning toward the east. High velocity field at the middle level indicates the entrainment of dry air from behind the storm. Mixing ratios of cloud-top, dry air, and incloud air have not been known.

When the tornado-downburst cycles are repeated, periodic formations of tornadoes take place. Refer to Fujita (1963), Darkow (1971), and Fujita (1974).

Figures 14 and 15 show an example of the transition from Stage 0 (but no tornado) to Stage 1 which took place over the Project NIMROD Network. In only 3 minutes, the echo top turned into an horseshoe-shaped configuration.

A series of velocity patterns superimposed upon reflectivity patterns in Figure 16 reveal the formation of a 30 DBZ hole atop the echo at about 12 km AGL. A pocket of 25 to 26 m/sec velocity toward CHL developed near the cloud top and descended all the way, nearly to the ground.

CP-3 radar at YKV pointed vertically for about 2 hours during the passage of this supercell and the second one which followed. A 28 m/s downward velocity at the 6 DBZ echo top was measured by the vertically pointing Doppler at 1642 CDT. Refer to Wilson and Fujita (1979) in this Preprint volume.

It is suspected that other supercells which produce tornadoes and twisting downbursts are going through this evolution cycle. Of course, each cloud may behave differently in terms of cycle periods, dimensions, and intensities.

Nevertheless, the existence of a downburst extending from the caved-in top down to the ground is likely to be the key feature of the proposed evolution.

Because of rapid changes in the cloud structure during the early downburst stage, the 3-minute scan cycle used during the NIMROD operation was not fast enough to determine the changes. The confirmation of the rapidly sinking cloud could not have been made without using the CP-3 antenna pointed up vertically.

6. CONCLUSIONS AND FUTURE RESEARCH

Current research on the NIMROD data has revealed that bow echoes and hook echoes are closely related to the formation of tornadoes and downbursts. Project NIMROD also has obtained the basic data of isolated downbursts, microbursts, and gust fronts.

The evidence and the mechanism of the long descent of the downburst air has been the focal point of the Kessler—Fujita controversy. Nonetheless, we, as long-time friends in search of severe storm mechanisms, equally believe that an effort in solving this type of disagreement does contribute to the advancement of the new knowledge sought by all storm researchers.

NIMROD network data can now be utilized for the α, β, γ, scale mesoanalyses. The data, when utilized with extreme care, now permit us to identify tornado-scale vortices. Signatures of three vortices, 40 to 100 m across, already have been analyzed. Refer to Wilson and Fujita (1979) in this Volume.

Foreseeing the improved capabilities of Doppler radars in the years to come, the original MESO scale was expanded upward into MASO and downward into MISO, MOSO, and MUSO scales in the reversed, alphabetic order of the vowels A, E, I, O, and U.

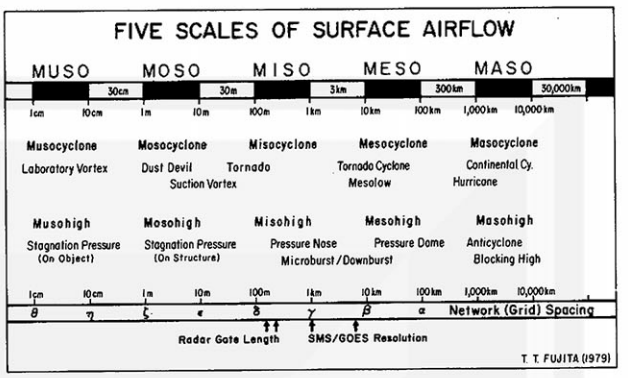

Both meso- and misoscale analyses of NIMROD data will continue for the next couple of years while we keep collecting the wind damage data on a nationwide scale. SESAME, 1979 data will be analyzed in an effort to compare the structure of storms in Oklahoma and in Illinois.

Acknowledgement:- Research supported by the Atmospheric Research Section, National Science Foundation, Grant No. ATM78-01074; NASA, Grant No. NGR 14-001-008; NESS, Grant No. 04-4-158-1; and NRC, Contract No. 04-74-239.

REFERENCES

Abbey, R. F., Jr. (1976): Risk probabilities associated with tornado windspeeds. Proc., Symp. on Tornadoes, Texas Tech. Univ., 177-236.

Brandes, E. A. (1978): Mesocyclone evolution and tornado generation within the Harrah, Oklahoma Storm. NOAA Tech Memo ERL-NSSL 81. Also see, Mesocyclone Evolution and Tornadogenesis: Some Observations. Mon. Wea. Rev., 106, 995-1011.

Brandes, E. A. (1977): Flow in severe thunderstorms observed by dual-Doppler radar. Mon. Wea. Rev., 105, 113-120.

Burgess, D. W., R. A. Brown, L. R. Lemon, and C. R. Safford (1977): Evolution of a tornadic thunderstorm. Preprint Vol., 10th Conf. on Severe Local Storms, 84-89.

Faust, H. (1947): Untersuchungen vor Forstschäden Hinsichtlich der Windstruktur bei einer B6. Meteor. Rundschau., 1, 290-297.

Forbes, G. S. (1977): Thunderstorm-scale variations of echoes associated with left-turn tornado families. Preprint Vol., 10th Conf. on Severe Local Storms, 497-504.

Fujita, T. T. (1971): Proposed characterization of tornadoes and hurricanes by area and intensity. SMRP Res. Paper 91, Univ. of Chicago, 42 pp.

Fujita, T. T. (1973): Proposed mechanism of tornado formation from rotating thunderstorms. Preprint Vol., 8th Conf. on Severe Local Storms, 191-196.

Fujita, T. T. and A. D. Pearson (1973): Results of FPP classification of 1971 and 1972 tornadoes. Preprints, 8th Conf. on Severe Local Storms, 142-145.

Fujita, T. T. (1976): Spearhead echo and downburst near the approach end of a John F. Kennedy Airport runway. SMRP Res. Paper 137, Univ. of Chicago, 51 pp.

Fujita, T. T. and H. R. Byers (1977): Spearhead echo and downburst in the crash of an airliner. Mon. Wea. Rev., 105, 129-146.

Fujita, T. T. and F. Caracena (1977): An analysis of three weather-related aircraft accidents. Bull. of Amer. Met. Soc., 58, 1164-1181.

Fujita, T. T. (1978): Manual of Downburst Identification for Project NIMROD. SMRP Res. Paper 156, Univ. of Chicago, 104 pp.

Goff, R. C. (1975): Thunderstorm-outflow kinematics and dynamics. NOAA Tech. Memo ERL-NSSL No. 75.

Hamilton, R. E. (1970): Use of detailed intensity radar data in mesoscale surface analysis of the July 4, 1969 storm in Ohio. Preprint Vol., 14th Radar Met. Conf., 339-346.

Lemon, L. R., D. W. Burgess, and R. A. Brown (1975): Tornado production and storm sustenance. Preprint Vol., 9th Conf. Severe Local Storms, 100-104.

Lemon, L. R. (1977): Severe thunderstorm evolution: Its use in a new technique for radar warnings. Preprint Vol., 10th Conf. on Severe Local Storms, 77-83.

Müldner, W. (1950): Die Windbruchschäden des 22.7.1948 im Reichswald bei Nürnberg, ein Beispiel für ein Wirbelfeld als Teilerscheinung einer Böenfront. Berichte des Deutschen Wetterdienstes in der U.S. Zone, 19, 3-39.

Nolen, R. H. (1959): A radar pattern associated with tornadoes. Bull. Amer. Met. Soc., 40, 277-279.

Ray, P. S., et al., (1975): Dual-Doppler observations of a tornadic storm. J. Appl. Met., 14, 1521-1530.

Ray, P. S. (1976): Vorticity and divergence fields within tornadic storms from dual-Doppler observations. J. Appl. Met., 15, 879-890.

Ray, P. S. (1978): Triple-Doppler observations of a convective storm. J. Appl. Met., 17, 1201-1212.